Biosensors and Bioelectronics 145 (2019) 111714

Contents lists available at ScienceDirect

Biosensors and Bioelectronics

journal homepage: www.elsevier.com/locate/bios

Simple and universal signal labeling of cell surface for amplified detection of cancer cells via mild reduction

Lingling Li[a,b], Bing Han[a], Ying Wang[a], Jing Zhao[a,**], Ya Cao[a,*]

[a] Center for Molecular Recognition and Biosensing, School of Life Sciences, Shanghai University, 200444, PR China
[b] Shanghai Key Laboratory of Bio-Energy Crops, Shanghai University, 200444, PR China

ARTICLE INFO

Keywords:
Mild reduction
Thiol-maleimide conjugation
DNA bridge
Silver nanoclusters
Electrochemical sensing
Cancer cell detection

ABSTRACT

Membrane protein, a novel surface biomarker, plays an important role in cell recognition and disease diagnosis. Accurate recognition of membrane protein ensure high specificity of cell identification, while introducing signal molecules onto cell membrane is critical to achieve high sensitivity. In this work, we introduced a simple and universal signal labeling approach for cancer cell detection based on mild reduction-mediated cell engineering. This approach included the mild reduction of disulfide bonds within membrane proteins and the introduction of DNA bridge complex-templated silver nanoclusters (DNA bridge-AgNCs) through the thiol-maleimide conjugation. The mild reduction reactions on the cell surface significantly increased the binding sites for signal labeling, and DNA bridge-AgNCs served as a scaffold of signal amplification, resulting in a wide linear range from 50–2×10^6 cells, and a detection limit of 15 cells. In addition, the method also showed good selectivity in complex environment. Therefore, this method may have great application space in the field of cell detection and even disease diagnosis in the near future.

1. Introduction

Cell membrane is a typical lipid bilayer embedded with diverse biomolecules. Cell membrane well maintains the integration of cell shape and structure, and thus protects the intracellular components from the interference of outside environment (Simons and Ikonen, 1997). As a kind of semipermeable membrane, cell membrane selectively regulates the transportation of different substances into or out of the cells, guaranteeing the cell survival and viability (Vogel and Sheetz, 2006). On the other hand, biological molecules that are incorporated into the membrane play a key role in performing natural functions for cell-cell or cell-extracellular communications (Loewenstein, 1981). Specially, membrane proteins, accounting for a large proportion of membrane volume, are responsible for different biological activities. Surface receptors take part in signal transduction between the cell and exterior environments, and can trigger cascade signal responses inside the cells upon extracellular stimuli (He and Tian, 2018), while integral proteins as amphipathic transmembrane channels facilitate the transportation of biological substances across the membrane for the maintenance of cellular homeostasis (Wu, 2013). Beside the native functions, membrane proteins are also emerged as a new type of surface biomarkers for cell identification and even disease diagnosis in recent decades, as their expressions constantly alter in response to changes of cellular states (Pollock et al., 2018; Song et al., 2015; Ullal et al., 2014). In this sense, plentiful membrane proteins are highlighted in cell identification, especially for the detection of cancer cells, such as epidermal growth factor receptor (EGFR) for lung cancer (Gainor et al., 2016), MUC1 for breast cancer (Maeda et al., 2018), and glypican-3 (GPC3) for liver cancer (Gao et al., 2015).

In general, accurate recognition of surface biomarkers ensure high selectivity and specificity of the detection of cancer cells, while high sensitivity of the biosensing methods are strongly rely on the signal intensity. In order to achieve high sensitivity, the modification of cell membrane is usually required for signal labeling as a critical precondition of signal obtaining (Shi et al., 2011; Tanenbaum et al., 2014). Two approaches are commonly used in the surface labeling. One is indirect labeling, in which signal molecules are linked to recognition ligands (e.g. antibody, aptamer and peptides) and bind to cell surface through the specific bio-affinity with membrane protein (Cao et al., 2019; Tang et al., 2019; Wang et al., 2016; Zhao et al., 2018). The other is direct labeling, in which signal molecules are directly immobilized onto the cell membrane through certain chemical linkages, such as the interaction between concanavalin A and mannosyl groups on cell surface glycoproteins, or the azide-alkyne cycloaddition between alkyne

* Corresponding author.
** Corresponding author.
E-mail addresses: jingzhao@t.shu.edu.cn (J. Zhao), conezimint@shu.edu.cn (Y. Cao).

https://doi.org/10.1016/j.bios.2019.111714
Received 26 July 2019; Received in revised form 5 September 2019; Accepted 17 September 2019
Available online 18 September 2019
0956-5663/

moiety and metabolically engineered membrane glycoproteins (Nikic et al., 2015; Wang et al., 2018). However, these labeling approaches have several limitations: indirect labeling could be easily influenced by steric hindrance upon molecular recognition and is usually lack of efficiency (Harper and Sigman, 2011); direct labeling typically results in unideal versatility and incomparable labeling yield for different cells because of the significant differences in glycosylation state (Zhang et al., 2019). In this context, developing a new signal labeling approach with high efficiency and universality is remarkably attractive.

Recently, mild reduction has emerged to be a promising tool in cell engineering (Cha et al., 2018; Custodio and Mano, 2016; Kim et al., 2018), in which disulfides of membrane protein were reduced to active thiols using a mild reducing agent tris(2-carboxyethyl)phosphine (TCEP). By further coupling a thiol-reactive signal molecules, mild reduction may offer a superior choice for signal labeling. On the one hand, since internal disulfide bonds play an important role in protein folding and stabilization, many membrane proteins are rich in disulfides (Metcalfe et al., 2011), and thereby can provide plentiful thiol sites once treated by TECP. This ensures the efficiency and yield of signal labeling. On the other hand, the wide source of membrane proteins containing disulfide bonds may help eliminate the incomparable labeling yield for different types of cells, making the signal labeling approach more universal.

Herein, we explore, for the first time, the potential function of mild reduction in signal labeling, and propose an amplified sensing method for the electrochemical detection of cancer cells using hepatocellular carcinoma (HCC) cells HepG2 as model. GPC3, an ideal surface biomarker for HCC that is overexpressed in HCC tissues and absent in normal tissues, cirrhotic liver, and benign lesions, was employed to recognize and capture target HepG2 cells with high selectivity (Li et al., 2014; Han et al., 2018; Zhu et al., 2016). In the work, a maleimide modified single-stranded oligonucleotide (maleimide-DNA) was designed for the labeling of cell surface after mild reduction, and a DNA bridge complex was designed as a scaffold to arouse signal generation and amplification. Scheme 1 illustrates the principle of the signal labeling approach and the method. First, 4-sulfocalix[4]arene hydrate (pSC_4), containing an electron-rich cavity structure, was modified on the surface of a gold electrode (GE) through Au–S interaction. pSC_4 could facilitate the orientation and immobilization of anti-GPC3 antibody through host-guest recognition and prepare a functional electrode (anti-GPC3/pSC_4/GE) (Chen et al., 2014). Secondly, target GPC3-positive HepG2 cells were pretreated with TCEP to expose active thiols and then captured onto the surface of the functional electrode via immune recognition. Thirdly, maleimide-DNA covalently bound to active thiol groups on cell surface to form thiol-maleimide conjugation through Michael addition reaction (Fontaine et al., 2015), which facilitated signal labeling by recruiting DNA bridge complex-templated silver nanoclusters (DNA bridge-AgNCs). Finally, the qualitative and quantitative information of target cells could be reflected by tracing the electrochemical responses of labeled AgNCs.

2. Experimental section

2.1. Chemicals and materials

pSC_4 was purchased from TCI Co., Ltd. (Shanghai, China). Anti-GPC3 antibody, anti-nucleonin (anti-NCL) antibody, anti-MUC1 antibody, and phalloidin-iFluor 488 were purchased from Abcam (Shanghai, China). Goat anti-rabbit IgG/FITC was purchased from Biosynthesis Biotechnology Co., Ltd. (Beijing, China). 3,3′-dioctadecyloxacarbocyanine perchlorate (Dio) was purchased from Beyotime Biotechnology Co., Ltd. Ammonium acetate (NH_4Ac), silver nitrate ($AgNO_3$), sodium borohydride ($NaBH_4$), bovine serum albumin (BSA), N-hydroxysuccinimide (NHS), N-(3-Dimethylaminopropyl)-N′-ethlcarbodiimide hydrochloride (EDC), 6-mercapto-1-hexanol (MCH) and TCEP were obtained from Sigma-Aldrich (Shanghai, China). Carboxylated magnetic beads and Ellman's reagent (5,5-dithio-bis-(2-nitrobenzoic acid) (DTNB)) were purchased from Invitrogen (Shanghai, China). HepG2, MCF-7, and L02 cells were purchased from the Institute of Biochemistry and Cell Biology of Chinese Academy of Science (Shanghai, China). High-glucose Dulbecco's modified Eagle medium (DMEM), fetal bovine serum (FBS) and penicillin-streptomycin-neomycin solution were purchased from Biological Industries Co., Ltd. (Israel). Normal human serum was obtained from AmyJet Scientific Inc. (Wuhan, China). All solutions were prepared with Milli-Q water (18.2 MΩ cm^{-1}) from a Milli-Q purification system (Milford, USA). All other chemicals were of analytical reagent grade. All DNA probes used in this research were synthesized and purified by Shanghai Sangon Biotechnology Co., Ltd. (Shanghai, China). Their sequences were listed in Table S1 in Supporting Information.

2.2. Synthesis of DNA bridge-AgNCs

Firstly, the DNA bridge complex (b1/b2/p1/p2) was prepared by

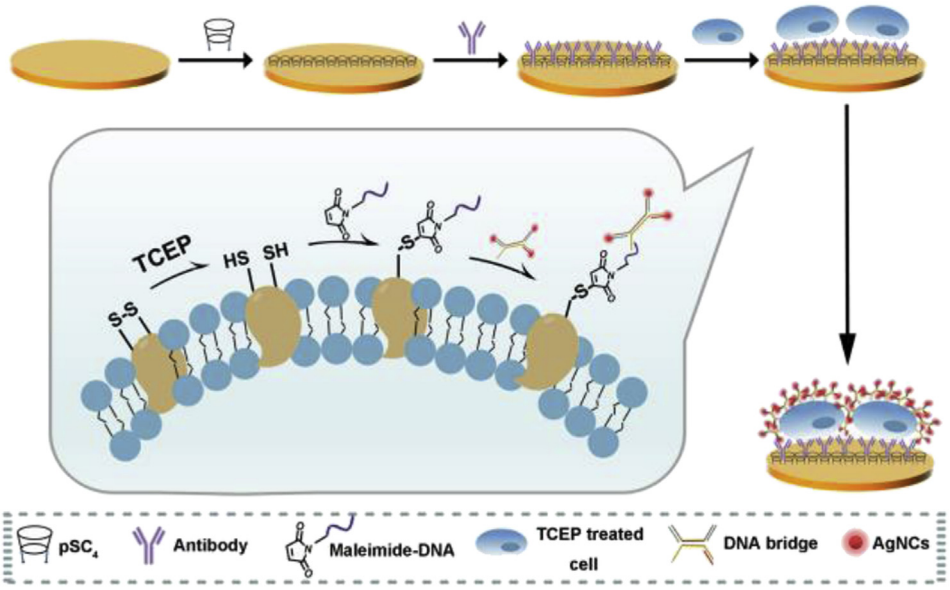

Scheme 1. Representation of the principle of signal labeling and electrochemical sensing of cancer cells via mild reduction.

mixing 2 μL of 100 μM DNA probe b1, b2, p1 and 4 μL of 100 μM DNA probe p2 in a centrifuge tube, and then being annealed at 95 °C for 5 min and naturally cooled to room temperate. After that, 95 μL of 100 μM $AgNO_3$ and 95 μL of 100 μM NH_4Ac were added into a 0.5 mL centrifuge tube, which were further mixed with 10 μL of the DNA bridge complex to form a solution with a total volume of 200 μL. After violent oscillation, the mixed solution was placed at 4 °C for 20 min in dark. Subsequently, 5 μL of 100 μM $NaBH_4$ aqueous solution (ice water) was added to the mixed solution. After being shaken violently, the mixed solution was protect from light at 4 °C for 2 h to achieve stable DNA bridge-AgNCs.

2.3. Cell culture and TCEP treatment

HepG2, MCF-7, and L02 cells were cultured in high-glucose DMEM medium containing 10% FBS, 1% penicillin-streptomycin-neomycin and collected at the end of the log phase. After being washed twice with PBS, cells at a concentration of 2×10^6 cells per mL were collected in 1.5-mL tube by centrifugation at 500 rpm and suspended in 1 mL of PBS containing 1 mM of TCEP. Then the samples were incubated at 37 °C for 20 min. After incubation, the cells were washed with PBS (2 mM Mg^{2+} in PBS) twice and dispersed at various concentrations. The amount of active thiols on cell surface was determined based on Ellman's reagent. Briefly, a 50-μL aliquot of Ellman's reagent and 2.5 mL of 0.1 M PBS (pH 8.0) was added into 250 μL of cells and incubated at 25 °C for 15 min. The absorbance was then recorded at 412 nm.

2.4. Cell imaging

To characterize the mild reduction and mediated signal labeling, TCEP-treated HepG2 and L02 cells were incubated with fluorophore-functionalized maleimide-DNA (maleimide-DNA*FAM) for 30 min, or incubated with maleimide-DNA for 30 min and DNA bridge-AgNCs for 1 h in sequence. To investigate the expression of GPC3 and the influence of mild reduction on immunoreaction, anti-GPC3 antibody was incubated with HepG2 and L02 cells (with or without TECP treatment) for 2 h, then blocked with 2% BSA for 15 min, and incubated with goat anti-rabbit IgG/FITC for 1 h. After that, cell nucleus was stained with Hoechst for 10 min. All the above reactions were carried out at 37 °C and rinsed twice with PBS after each reaction. Fluorescent images were finally obtained using a LSM 710 confocal laser scanning microscope (Zeiss, Germany).

2.5. Cell capture using antibody functionalized magnetic beads

To prepare antibody functionalized magnetic beads (anti-GPC3/MBs), 1 mL of 0.2 M EDC and 0.1 M NHS were first added to 100 μL of 10 mg/mL carboxylated magnetic bead solution. After activation for 1 h at 25 °C, the magnetic beads were rinsed with deionized water for 3 times. Then, the magnetic beads were suspended with 500 μL PBS containing 100 μg anti-GPC3 antibody at 25 °C for 2 h, followed by being blocked with 10 mg/mL BSA for 1 h. For cell capture, the prepared anti-GPC3/MBs were incubated with TCEP pretreated cells for 2 h at 37 °C and then rinsed three times with PBS. After magnetic separation, the captured cells were stained with 30 μM DiO for 30 min at 37 °C. The fluorescent images were obtained by Zeiss Axio Imager M2 fluorescent microscopy (Zeiss, Germany).

2.6. Preparation of anti-GPC3/pSC_4/GE

GE was first pretreated according to previous literature (Zhao et al., 2018). Then, the electrode was incubated with 1 mM pSC_4 overnight and then treated in 1 mM MCH solution for 1 h to block the non-specific site, followed by incubating with anti-GPC3 antibody for 2 h at 4 °C.

2.7. Signal labeling and electrochemical detection of cells

Cell capture by electrode was obtained by inserting anti-GPC3/pSC_4/GE into a solution containing different concentrations of TCEP-treated cell at 37 °C for 2 h, and then washed with PBS twice. Then, the electrode was immersed into 100 μL of PBS containing 1 μM maleimide-DNA at 37 °C for 30 min and washed twice by PBS. After then, the electrode was immersed into 200 μL of DNA bridge-AgNCs or single-stranded DNA probe b1' templated AgNCs (Single AgNC) at 37 °C for 1 h. In control experiments, the electrode was immersed into 100 μL of PBS containing 1 μM single stranded DNA probe (NCL probe) instead of maleimide-DNA at 37 °C for 30 min and washed twice by PBS. After then, the electrode was immersed into 200 μL of DNA bridge-AgNCs at 37 °C for 1 h to form the Aptamer bridge-AgNCs. After rinsing with PBS, the electrode was placed in a solution of 0.5 M HNO_3 and reacted for 2 h at room temperature. Afterward, the resulting solution was transferred into sodium acetate buffer and the amount of dissolved silver ions (Ag^+) was then electrochemically determined.

Electrochemical measurements were conducted on a CHI-660c electrochemical workstation (CH Instruments) with a conventional three-electrode system. Electrochemical impedance spectra (EIS) were recorded by using $[Fe(CN)_6]^{3-/4-}$ as the redox probe. Differential pulse voltammetry (DPV) responses were measured after an 8-min electrodeposition of Ag^+ at −1.2 V. The potential range and amplitude for DPV measurements were −0.1–0.5 V and 25-mV respectively. All measurements were conducted at least three times.

3. Results and discussion

3.1. Characterization of mild reduction and thiol-maleimide conjugation

In order to demonstrate the generation of active thiols at cell surface after mild reduction, Ellman's reagent was used to quantify active thiols before and after TCEP treatment. Ellman's reagent is able to react with active thiols to yield a mixed disulfide and 2-nitro-5-thiobenzoic acid which has a maximum absorption peak at 412 nm (Riddles et al., 1979). Fig. 1A shows the Ellman's assay results for HepG2 cells. Obviously, the absorption peak at 412 nm was significantly increased after TCEP treatment, compared to that without TCEP treatment, suggesting the produce of a large number of active thiols on the cell surface. Also, we designed a FAM-functionalized maleimide-DNA (maleimide-DNA*FAM) to reveal the occurrence of mild reduction and thiol-maleimide conjugation. As shown in Fig. 1B, obvious green fluorescence was observed after incubation of maleimide-DNA*FAM with TCEP-treated cells (both HepG2 and normal liver cells L02). In comparison, nearly no fluorescence was observed in the cases without TCEP treatment or the cases using FAM-functionalized DNA (DNA*FAM) instead of maleimide-DNA*FAM. The results clearly demonstrated that active thiols were successfully generated on cell surface via mild reduction and linked to maleimide-DNA through Michael addition reaction in spite of cell types. A weak fluorescence for the case without TECP treatment may attribute to inherent active thiol groups at cell surface, corresponding to the control results of a slight increase of absorbance in Fig. 1A.

Effect of mild reduction on cell morphology, which was critical for the following signal labeling and detection, was also investigated. As shown in Fig. S1, TCEP treatment cause no adverse effect on cell morphology, especially no obvious breakage of cell membrane. Afterward, the influence of mild reduction toward immunoreaction activity of membrane protein was studied. To this end, HepG2 and L02 cells were firstly incubated with anti-GPC3, and then reacted with FITC-labeled secondary antibody for indirect labeling. Fig. 1C displays the obtained fluorescent images, in which very bright green fluorescence was shown in the presence of HepG2 cells no matter whether they were treated with TCEP, while nearly no fluorescence was observed in the presence of L02 cells. In addition, Fig. 1D shows the results of specific

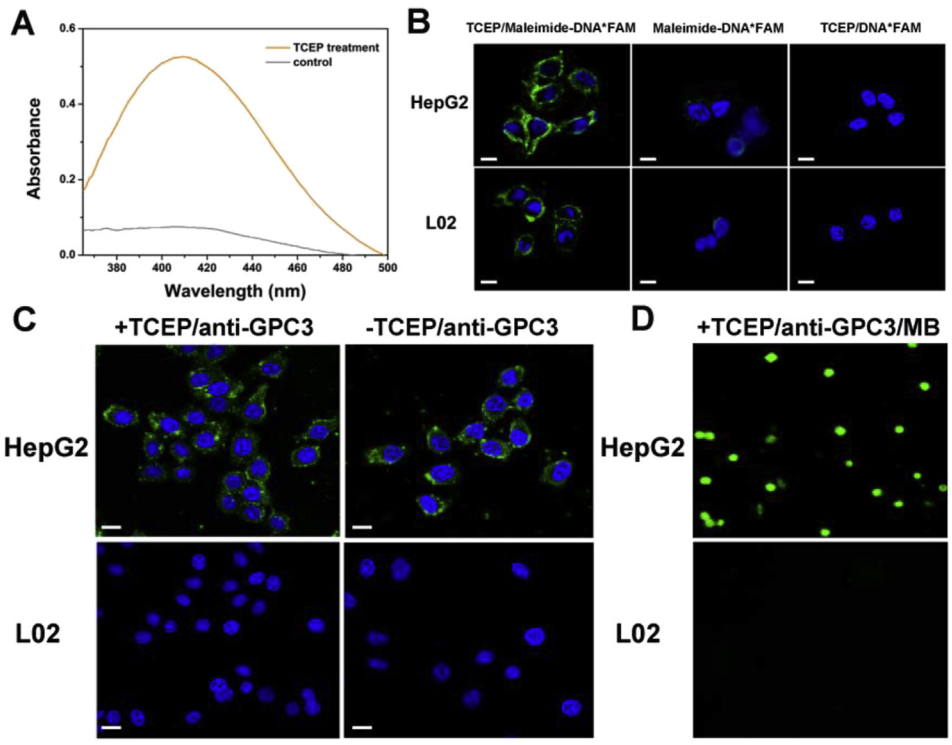

Fig. 1. (A) Ellman's assay results for HepG2 cell with/without TCEP treatment. (B) Confocal images of HepG2 and L02 cells treated with TCEP and maleimide-DNA*FAM (left), maleimide-DNA*FAM (middle), or TCEP and DNA*FAM (right). Scale bar represents 20 μm. (C) Confocal imaging of GPC3 on HepG2 and L02 cells with/without TCEP treatment. Scale bar represents 20 μm. (D) Fluorescence microscopy images of cells captured by anti-GPC3/MBs.

cell capture using anti-GPC3/MBs. The captured cells were stained by membrane stainer DiO, which can gradually stain the membrane of whole cell and present bright green fluorescence (Honig and Hume, 1989). After magnetic separation, strong green fluorescence was observed at anti-GPC3/MBs in the presence of TECP-treated HepG2 cells, while no fluorescence was observed in the presence of TECP-treated L02 cells. Both results agree with the fact that membrane protein GPC3 is highly expressed on HepG2 but lowly expressed on L02 cells, and suggests that mild reduction has no negative effect on the amounts and immunoreaction activities of surface protein. Overall, the above studies demonstrate that active thiol groups could be successfully produced on the TCEP-treated cell surface and feasibly bound with maleimide-DNA through thiol-maleimide conjugation, which had nearly no effect on cell morphology and immunoreaction activity.

3.2. Validation of DNA bridge-AgNCs

In the work, a DNA bridge complex was designed to be the template for AgNCs synthesis and a scaffold to arouse signal generation. So, the preparation and usability of DNA bridge complex and templated AgNCs were validated. Agarose gel electrophoresis was carried out to demonstrate the formation of DNA bridge complex (Fig. S2A), and TEM image was recorded to characterize the synthesized AgNCs using DNA bridge complex as template (Fig. S2B). Fig. S2C shows the fluorescence responses of DNA bridge-templated AgNCs. A bright fluorescence was observed with the maximum fluorescence emission peak at 632 nm. Fig. S2D shows confocal images of HepG2 and L02 cells using DNA bridge-AgNCs as signal labels. In this case, HepG2 and L02 cells were first treated with TCEP, and then incubated with maleimide-DNA and DNA bridge-AgNCs in sequence. Strong red fluorescence was observed in the presence of both cells after TCEP treatment, which was as expected. The results not only confirm the usability of DNA bridge-AgNCs as signal reporters but also demonstrate the feasibility and universality of mild reduction-mediated signal labeling on cell surface.

3.3. EIS characterization of cancer cell capture and signal labeling

Electrochemical techniques have received increasing attention in the early diagnosis of cancers, benefiting from the advantages of simple operation, low cost, high sensitivity and excellent accuracy (Ding et al., 2018; Gao et al., 2019; Jeong et al., 2016). So, we transferred the mild reduction-mediated signal labeling approach to an electrochemical sensing method for cancer cell detection using HepG2 cell as model. Fig. 2A illustrates the schematic diagram of stepwise surface reaction at the GE. Fig. 2B shows impedance results in the presence of TCEP-treated HepG2 cells. Impedance value gradually increased with the assembly of pSC_4 (curve b) and anti-GPC3 (curve c), the capture of TCEP-treated HepG2 cells (curve d) and the label of DNA bridge-AgNCs (curve e). This would attribute to progressively increased steric hindrance and negative charges, which was reasonable based on the principle of our method. Fig. 2C shows impedance results in the presence of HepG2 cells without TCEP treatment. The results are in line with our expectations. HepG2 cells were captured on anti-GPC3/pSC_4/GE through overexpressed membrane protein GPC3. However, without TCEP treatment, maleimiede-DNA was almost unable to be immobilized onto the cell surface for the lack of active thiol groups, and thus inhibited the labeling of DNA bridge-AgNCs. Fig. 2D shows impedance values in the presence of L02 cells with TCEP treatment. Nearly no changes of impedance values was observed after preparation of anti-GPC3/pSC_4/GE. The comparison with that in the presence of HepG2 demonstrated that target cells was successfully identified by using surface antigen GPC3, which coincided with the fluorescent studies on magnetic beads. Overall, EIS studies demonstrated the feasibly of our method that could be used for the further electrochemical detection.

3.4. Electrochemical detection of cancer cells based on mild reduction-mediated signal labeling

DNA bridge-AgNCs that labeled on cell surface could be electrochemically measured, which in turn enabled detection of target cells. Fig. S3 presents a typical DPV signal of DNA bridge-AgNCs with a peak potential of 0.18 V, which is ascribed to the oxidation of silver at the

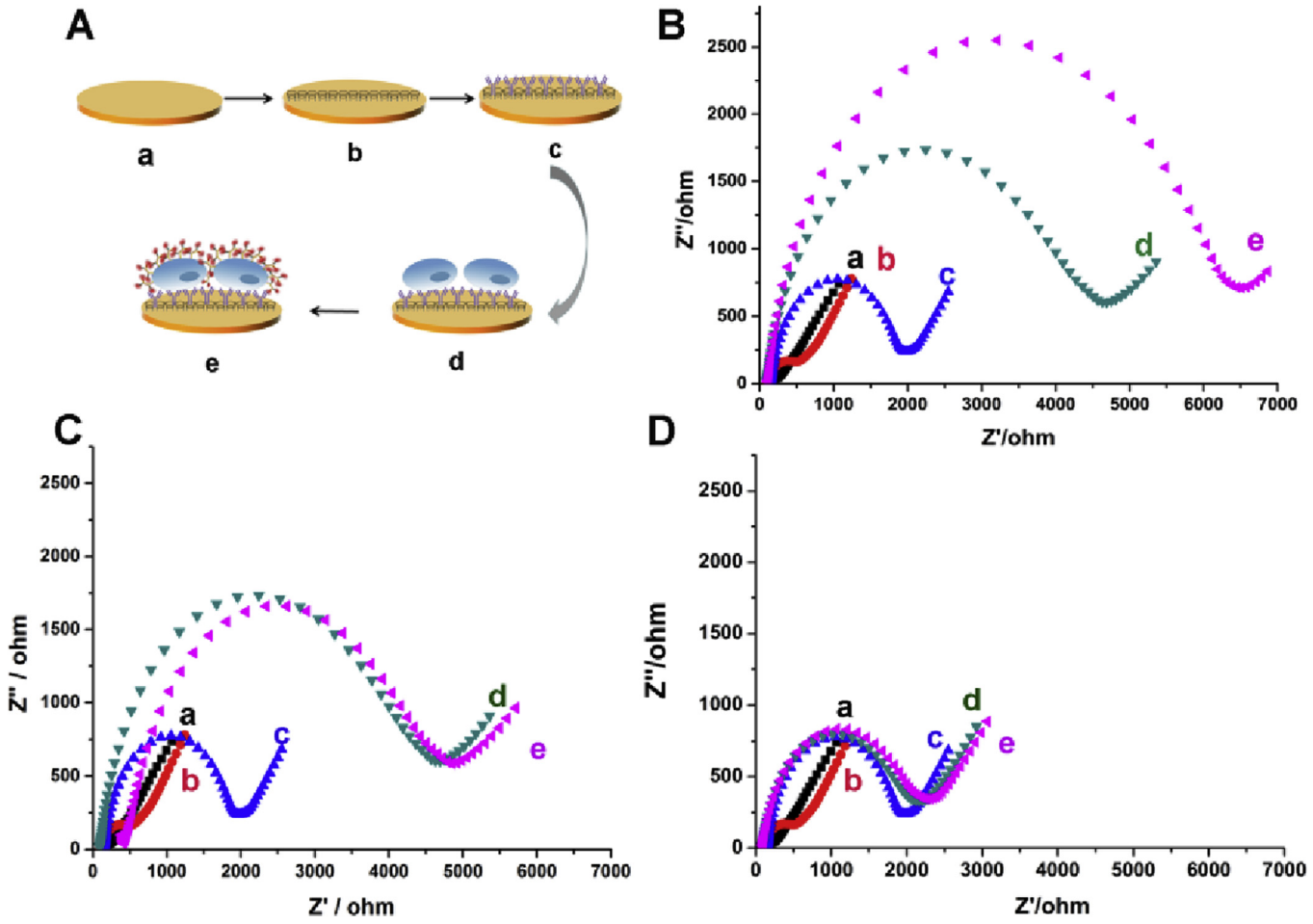

Fig. 2. Schematic illustration (A) and impedance results of step-by-step reaction at the GE, which correspond to (B) HepG2 cells with TCEP treatment, (C) HepG2 cells without TCEP treatment, and (D) L02 cells with TCEP treatment. (a) bare GE, (b) pSC_4-modified GE (pSC_4/GE), (c) anti-GPC3/pSC_4/GE, (d) cell/anti-GPC3/pSC_4/GE, and (e) DNA bridge-AgNCs/maleimiede-DNA/cell/anti-GPC3/pSC_4/GE. Electrolyte: 5 mM $[Fe(CN)_6]^{3-/4-}$.

electrode. Considering the excellent electrochemical performance of AgNCs, we employed DPV to reveal the responses in the presence of target cells. Fig. 3A shows DPV responses in the presence of different cells. A high peak current was obtained in the presence of HepG2 cells (curve a), while quite low electrochemical responses were obtained in the presence of control L02 cells (curve b) or in the absence of cells (curve c). The results confirm the high feasibility and selectivity of our method. Fig. 3B shows DPV responses under different reaction conditions in the presence of HepG2 cells. A high peak current was observed after TCEP treatment with the addition of maleimide-DNA (curve a), while quite low peak currents were observed without maleimide-DNA (curve b) or TECP treatment (curve c). The results reconfirm the detection procedure of our method. Mild reduction facilitates the generation of active thiol groups on the cell surface, and subsequently recruits maleimide-DNA and DNA bridge-AgNCs for signal labeling and reporting.

It should be noted that the employment of mild reduction and DNA bridge complex may also be beneficial to achieve desirable signal amplification. To demonstrate this, the electrochemical responses with the addition of 1×10^6 HepG2 cells were studied under three different conditions. As shown in Fig. 3C, a high electrochemical response was obtained in the presence of maleimide-DNA and DNA bridge-AgNCs for TCEP-treated HepG2 cells (curve a). However, once a single-stranded DNA probe b1' templated AgNCs (Single AgNC) was used instead of the DNA bridge-AgNCs, as depicted in Fig. S4, a much lower electrochemical response was obtained (curve b). The comparison demonstrate signal amplification from DNA bridge complex, which may carry triple signal molecules compared to single-stranded DNA probe. In another condition, a given membrane protein-targeted signal labeling approach was performed instead of mild reduction. NCL, a ubiquitous protein in eukaryotic cells that was proved to be highly expressed on the membrane of HepG2 cells (Fig. S5), was used as the model target. In this case, NCL probe containing a sequence of NCL aptamer and a complementary sequence to DNA bridge-AgNCs were designed to replace TCEP treatment and maleimide-DNA (Fig. S6). As expected, NCL probe, which can recognize and bind to NCL on the cell surface and then hybridize with DNA bridge-AgNCs to form Aptamer bridge-AgNCs, induced the lowest electrochemical response (curve c). The comparison with that using mild reduction indicated inherent signal amplification function of mild reduction because it can produce a large number of active thiols for labeling in spite of protein types. Fig. 3D shows the corresponding variation of peak current ($\Delta Q = I/I_{Blank}$) of different numbers of HepG2 cells under these three conditions. It also highlights that the method we designed has a great signal amplification effect.

Fig. 4A shows the quantitative results in the presence of different numbers of HepG2 cells. Peak currents were found to increase with addition of target cells, and the current signal became saturated when the number of cells reached 2×10^6 cells. Fig. 4B shows the relationship between the peak current and the number of cells. The inset further shows a good linear relationship between the peak current and the logarithm of HepG2 cell number from 50 to 1×10^6 cells. The regression equation is I (μA) = 0.829*lgCell* - 0.961 (R^2 = 0.994). The limit of detection (LOD) is calculated to be 15 cells. Compared with existing detection methods of HCC cells, the dynamic range and LOD of this

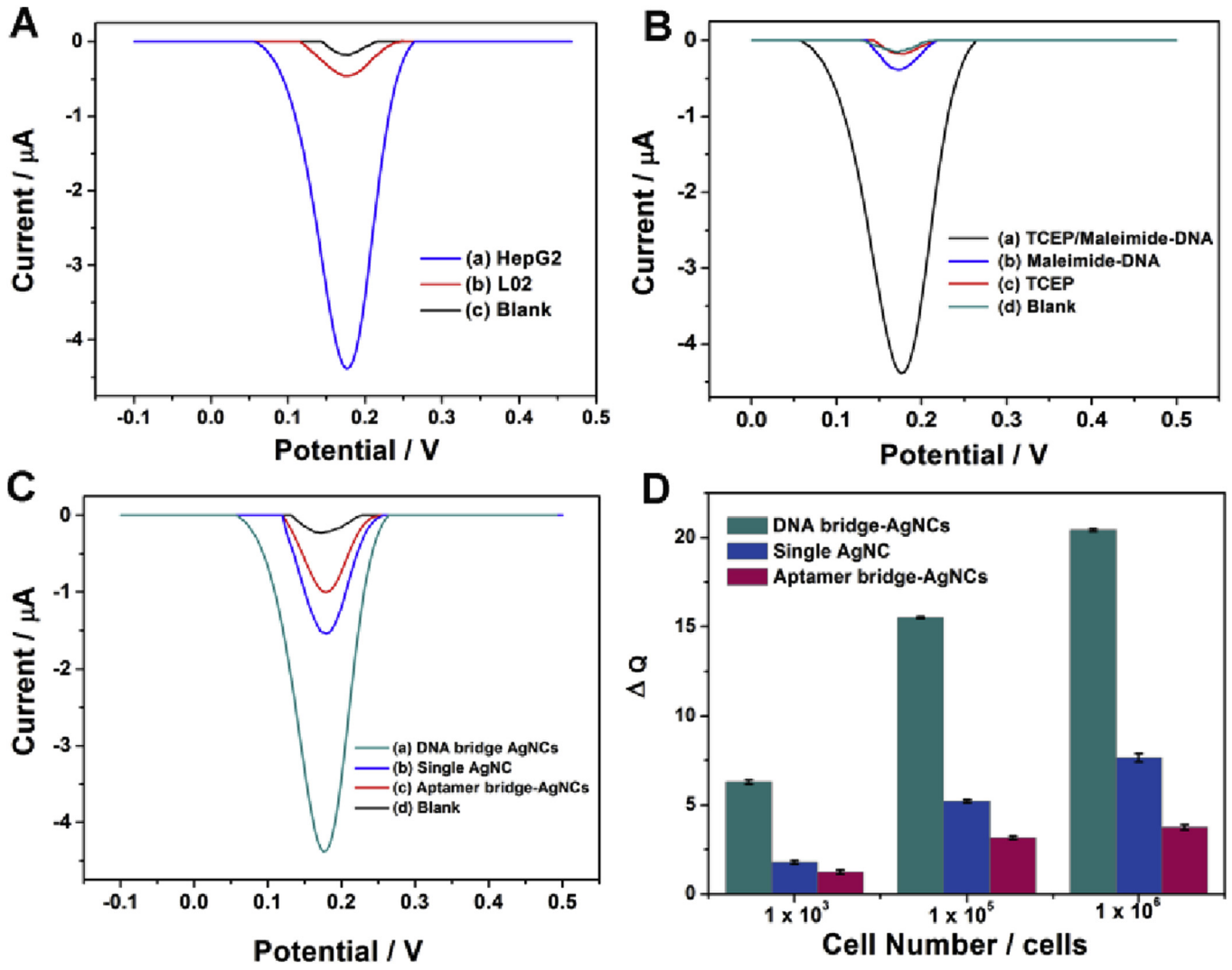

Fig. 3. (A) DPV responses in the presence of 1×10^6 (a) HepG2 and (b) L02 cells or (c) in the absence of cells (blank control) after incubation with DNA bridge-AgNCs. (B) DPV responses for 1×10^6 HepG2 cells with treatment of (a) TCEP and maleimide-DNA, (b) TCEP, or (c) maleimide-DNA. Curve d indicates the DPV response for blank control. (C) DPV responses for 1×10^6 HepG2 cells with the treatment of (a) TCEP, maleimide-DNA and DNA bridge-AgNCs, (b) TCEP, maleimide-DNA and Single AgNC, or (c) NCL probe and DNA bridge-AgNCs. Curve d indicates the DPV response for blank control. (D) Corresponding variation of peak current ($\Delta Q = I/I_{Blank}$) of different numbers of HepG2 cells under three conditions.

method are comparable or even better (Table S2), which would attribute to the employment of mild reduction and DNA bridge complex. Moreover, at least three measurements were repeated for each number of target cells, and the relative standard deviations (RSDs) were all within 10%. The average RSD value was 4.75%, indicating good reproducibility of our method.

To demonstrate the potential application of our method in the identification of HCC cells in a complex environment, different numbers of HepG2 cells were added to the 10% human serum samples. Fig. 5 shows the comparison of peak currents in the buffer with that in the serum sample. Obviously, peak currents with the addition of different numbers of HepG2 in PBS were all comparable to those in the serum environment. The experimental results reveal that HepG2 cells could be detected in human serum samples with good accuracy, suggesting the potential use of our method in clinical practice.

Finally, we investigated the universality of the signal labeling approach and the method by detecting breast cancer cell MCF-7 with the same procedure. It is reported that mucin 1 (MUC1) is highly expressed on MCF-7 cell surface (Chen et al., 2018). So, we replaced anti-GPC3 antibody with anti-MUC1 antibody to functionalize the GE and capture MCF-7 cells. As shown in Fig. S7, the electrochemical response is weak for blank control but is continuously increasing with MCF-7 cell number, demonstrating that the signal labeling can also take place on MCF-7 cell surface and the method can also be used for MCF-7 cell detection. Cross-reactivity experiments show that different peak currents can be obtained for HepG2 and MCF-7 cells using anti-GPC3 antibody and anti-MUC1 antibody respectively (Fig. S8). These data are in accordance with the distinct levels of GPC3 and MUC1 expression on the two cells (Chen et al., 2018; Pang et al., 2018), indicating desirable specificity.

4. Conclusions

To sum up, we designed a simple and universal signal labeling approach for cell analysis based on the guidance of TCEP-mediated mild reduction on cell membrane. Antibody functionalized electrode achieves specific capture of target cells through immune recognition, and DNA bridge-AgNCs can be immobilized onto cell surface after mild reduction-assisted conjugation with maleimide-DNA, thereby realizing signal labeling and amplification from triple bridge structure. Compared to the conventional labeling method, the mild reduction in spite of protein types can contribute to the enhanced labeling efficiency

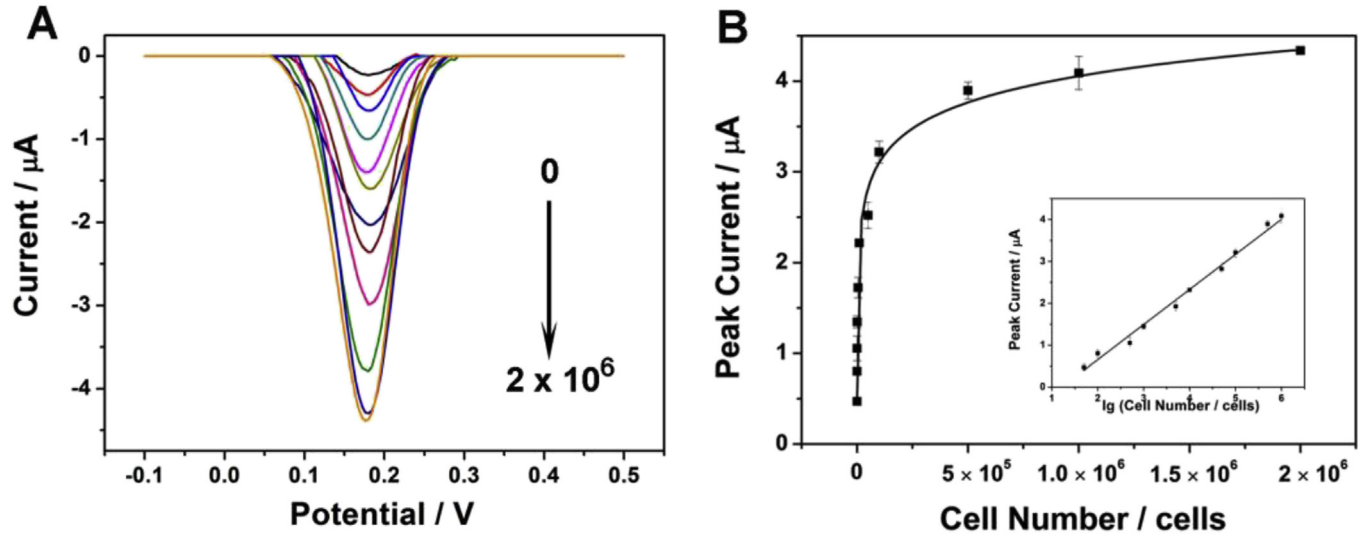

Fig. 4. (A) DPV responses with the addition of different number of HepG2 cells: 0, 50, 1×10^2, 5×10^2, 1×10^3, 5×10^3, 1×10^4, 5×10^4, 1×10^5, 5×10^5, 1×10^6, and 2×10^6 cells. (B) DPV peak current versus different cell numbers. Insert: The linear relationship between peak current values and the logarithmic values of cell numbers.

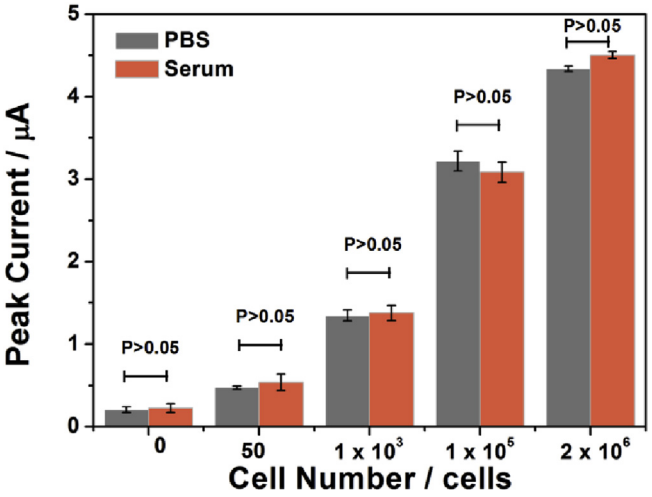

Fig. 5. Electrochemical results of different number of HepG2 cells obtained from the PBS and 10% human serum samples.

as well as the detection sensitivity. The experiments also demonstrate that our method can achieve a satisfactory specificity by using specific surface proteins as target, which is highly selective even in a complex serum environment. Therefore, our method may have a potential extensive use in the cell-related analysis by simply changing the recognition elements. Certainly, our method also has some shortcomings. For instance, the LOD is still higher than the need for quantification of HCC circulating tumor cells in peripheral blood (1–10 cells per milliliter) (Pang et al., 2018). To solve this problem, DNA-based amplification strategies, such as DNAzyme and catalytic hairpin assembly, may be employed to replace the DNA bridge, which is an ongoing subject of interest in our lab.

CRediT authorship contribution statement

Lingling Li: Writing - original draft, Writing - review & editing. **Bing Han:** Formal analysis, Writing - original draft, Writing - review & editing. **Ying Wang:** Formal analysis, Writing - original draft, Writing - review & editing. **Jing Zhao:** Supervision, Writing - original draft, Writing - review & editing. **Ya Cao:** Supervision, Writing - original draft, Writing - review & editing.

Declaration of competing interest

The authors declare that they have no known competing financial interests or personal relationships that could have appeared to influence the work reported in this paper.

Acknowledgments

This work was supported by the National Natural Science Foundation of China (Grant Nos. 81871449, 81671781, 81972799, and 81401489).

Appendix A. Supplementary data

Supplementary data to this article can be found online at https://doi.org/10.1016/j.bios.2019.111714.

References

Cao, Y., Dai, Y., Chen, H., Tang, Y., Chen, X., Wang, Y., Zhao, J., Zhu, X., 2019. Biosens. Bioelectron. 130, 132–138.
Cha, J., Kim, H., Hwang, N.S., Kim, P., 2018. ACS Appl. Mater. Interfaces 10, 35676–35680.
Chen, H., Liu, F., Qi, F., Koh, K., Wang, K., 2014. Int. J. Mol. Sci. 15, 5496–5507.
Chen, X.X., Zhao, J., Chen, T.S., Gao, T., Zhu, X.L., Li, G.X., 2018. Theranostics 8, 1075–1083.
Custodio, C.A., Mano, J.F., 2016. ChemNanoMat 2, 376–384.
Ding, S., Gu, Z., Yan, R., Tang, Y., Miao, P., 2018. Anal. Chim. Acta 1029, 24–29.
Fontaine, S.D., Reid, R., Robinson, L., Ashley, G.W., Santi, D.V., 2015. Bioconjug. Chem. 26, 145–152.
Gainor, J.F., Shaw, A.T., Sequist, L.V., Fu, X., Azzoli, C.G., Piotrowska, Z., Huynh, T.G., Zhao, L., Fulton, L., Schultz, K.R., Howe, E., Farago, A.F., Sullivan, R.J., Stone, J.R., Digumarthy, S., Moran, T., Hata, A.N., Yagi, Y., Yeap, B.Y., Engelman, J.A., Mino-Kenudson, M., 2016. Clin. Cancer Res. 22, 4585–4593.
Gao, T., Li, L., Chen, T., Shi, L., Yang, Y., Li, G., 2019. Anal. Chem. 91, 1126–1132.
Gao, W., Tang, Z., Zhang, Y.F., Feng, M., Qian, M., Dimitrov, D.S., Ho, M., 2015. Nat. Commun. 6, 6536.
Han, H.H., Qiu, Y.J., Shi, Y.Y., Wen, W., He, X.P., Dong, L.W., Tan, Y.X., Long, Y.T., Tian, H., Wang, H.Y., 2018. Theranostics 8, 3268–3274.
Harper, K.C., Sigman, M.S., 2011. Science 333, 1875–1878.
He, X.P., Tian, H., 2018. Chem 4, 246–268.
Honig, M.G., Hume, R.I., 1989. Trends Neurosci. 12, 333–341.
Jeong, S., Park, J., Pathania, D., Castro, C.M., Weissleder, R., Lee, H., 2016. ACS Nano 10, 1802–1809.
Kim, H., Shin, K., Park, O.K., Choi, D., Kim, H.D., Baik, S., Lee, S.H., Kwon, S.H., Yarema, K.J., Hong, J., Hyeon, T., Hwang, N.S., 2018. J. Am. Chem. Soc. 140, 1199–1202.
Li, Z., Zeng, Y., Zhang, D., Wu, M., Wu, L., Huang, A., Yang, H., Liu, X., Liu, J., 2014. J. Mater. Chem. B 2, 3686–3696.
Loewenstein, W.R., 1981. Physiol. Rev. 61, 829–913.

Maeda, T., Hiraki, M., Jin, C., Rajabi, H., Tagde, A., Alam, M., Bouillez, A., Hu, X., Suzuki, Y., Miyo, M., Hata, T., Hinohara, K., Kufe, D., 2018. Cancer Res. 78, 205–215.
Metcalfe, C., Cresswell, P., Ciaccia, L., Thomas, B., Barclay, A.N., 2011. Open Biol. 1, 110010.
Nikic, I., Kang, J.H., Girona, G.E., Aramburu, I.V., Lemke, E.A., 2015. Nat. Protoc. 10, 780–791.
Pang, Y.F., Wang, C., Xiao, R., Sun, Z.W., 2018. Chem. Eur J. 24, 7060.
Pollock, S.B., Hu, A., Mou, Y., Martinko, A.J., Julien, O., Hornsby, M., Ploder, L., Adams, J.J., Geng, H., Muschen, M., Sidhu, S.S., Moffat, J., Wells, J.A., 2018. Proc. Natl. Acad. Sci. U.S.A. 115, 2836–2841.
Riddles, P.W., Blakeley, R.L., Zerner, B., 1979. Anal. Biochem. 94, 75–81.
Shi, H., He, X., Wang, K., Wu, X., Ye, X., Guo, Q., Tan, W., Qing, Z., Yang, X., Zhou, B., 2011. Proc. Natl. Acad. Sci. U.S.A. 108, 3900–3905.
Simons, K., Ikonen, E., 1997. Nature 387, 569–572.
Song, X., Airan, R.D., Arifin, D.R., Bar-Shir, A., Kadayakkara, D.K., Liu, G., Gilad, A.A., van Zijl, P.C., McMahon, M.T., Bulte, J.W., 2015. Nat. Commun. 6, 6719.
Tanenbaum, M.E., Gilbert, L.A., Qi, L.S., Weissman, J.S., Vale, R.D., 2014. Cell 159, 635–646.
Tang, Y., Dai, Y., Huang, X., Li, L., Han, B., Cao, Y., Zhao, J., 2019. Anal. Chem. 91, 7531–7537.
Ullal, A.V., Peterson, V., Agasti, S.S., Tuang, S., Juric, D., Castro, C.M., Weissleder, R., 2014. Sci. Transl. Med. 6, 219ra219.
Vogel, V., Sheetz, M., 2006. Nat. Rev. Mol. Cell Biol. 7, 265–275.
Wang, J., Wang, X., Tang, H., Gao, Z., He, S., Li, J., Han, S., 2018. Biosens. Bioelectron. 100, 1–7.
Wang, R., Lu, D., Bai, H., Jin, C., Yan, G., Ye, M., Qiu, L., Chang, R., Cui, C., Liang, H., Tan, W., 2016. Chem. Sci. 7, 2157–2161.
Wu, H., 2013. Cell 153, 287–292.
Zhang, J., Chen, H., Cao, Y., Feng, C., Zhu, X., Li, G., 2019. Anal. Chem. 91, 1005–1010.
Zhao, J., Tang, Y., Cao, Y., Chen, T., Chen, X., Mao, X., Yin, Y., Chen, G., 2018. Electrochim. Acta 283, 1072–1078.
Zhu, D., Qin, Y., Wang, J., Zhang, L., Zou, S., Zhu, X., Zhu, L., 2016. Bioconjug. Chem. 27, 831–839.